ECS Transactions, 33 (4) 573-580 (2010)
10.1149/1.3483549 ©The Electrochemical Society

Characterization of Hysteresis of Surface Energy in Room-Temperature Direct Bonding Processes

David S. Grierson and Kevin T. Turner

Department of Mechanical Engineering, University of Wisconsin
Madison, WI 53706 USA

Room temperature direct wafer bonding is driven by surface forces and the formation of hydrogen bonds that pull the wafers being bonded into intimate contact. The magnitude of these forces is often represented as a work of adhesion, and is critical as it determines the level of non-flatness and patterning that may be tolerated in bonding. Traditionally, it has been assumed that the work of adhesion that drives the formation of the bond is equal to the work of separation that is measured through fracture tests, such as the familiar razor-blade test. In the present work, we use a novel test structure to measure both the work of separation and the work of adhesion of room temperature hydrophilic Si-Si bonds as a function of relative humidity (~15 – 50% RH). The results show that across a range of values of RH, the work of adhesion is significantly lower than the work of separation.

Introduction

Direct wafer bonding is an important process that enables the fabrication of a wide range of micro- and nanosystems (1). This process is commonly used in the fabrication of SOI substrates (2) and complex multi-wafer MEMS devices (3). In direct bonding, initial adhesion between the wafers is typically achieved at room temperature via van der Waals forces and hydrogen bonding. The strength of the adhesion is commonly described in terms of a single parameter, the work of adhesion (W_{adh}). The work of adhesion of bonded wafer pairs is most commonly measured with the razor-blade test (4), which is essentially a fracture test. The value of work of adhesion measured in the test is truly a work of separation value, rather than a work of adhesion value. Here, we measure both the work of adhesion and work of separation to establish if they are equal to one another in room temperature silicon direct bonding.

Previous researchers have used microfabrication techniques to develop measurement schemes for studying stiction between polycrystalline silicon beams and silicon substrates with various surface coatings as a function of humidity [(5, 6), for example]. These techniques have proven to be beneficial in understanding adhesion between micromachined surfaces, but are limited in their ability to fully characterize the adhesion and separation behavior bonded interfaces directly, and the range of material pairs is also limited.

The novel measurement approach detailed here is similar to the previous micromachined beam studies reported previously, but is distinct in that the beams are not

integrated with the test substrate. This apparatus is designed to hold an array of microfabricated beams at a slight angle (~0.2 degrees) above a surface and precisely control the separation between the beams and the substrate. Using an interferometric microscope to optically observe the deformed beams, a full characterization of the bonded interface can be achieved by calculating the strain energy release rate, *G*, as the beams contact and separate from the test substrate. In this work we present measurements of the work of adhesion and the work of separation between Si surfaces with a native oxide as a function of relative humidity (RH).

Experimental Methods

Test apparatus

A novel test apparatus was constructed to test both advancing and receding microscale adhesive contacts under controlled environmental conditions (Figure 1). The setup is operated by positioning and aligning an array of inclined micromachined beams above a test substrate, bringing the beams into adhesive contact with the substrate (with the formation of the bonding being driven solely by surface forces), and controllably pulling the beams away from the substrate (Figure 2). A Mirau interferometer is used to measure the deformed profiles of the beams continuously during a test. An adhesion-separation test consists of continuously monitoring the deformation behavior of the beams as they are brought both closer to and farther from the substrate. The work of adhesion and work of separation are measured by characterizing the deformed profiles of the beams, using a fracture mechanics framework (described subsequently), during receding and advancing portions of a test, respectively.

For this study, all contacts were hydrophilic single-crystal Si-Si contacts (details are provided in the Specimen Fabrication and Preparation section), and the environment was controlled by setting the RH at either ~15 or ~50% with nitrogen as the background gas. A complete test is conducted as follows. First, the beams are brought into adhesive contact with the test substrate, and the beams are held at a constant separation gap (s ~ 1 μm) for ~20 minutes while the deformed profiles are being recorded (henceforth referred to as a hold test). Following the first hold test, an adhesion-separation test (henceforth referred to as a ramp test) is conducted, whereby the separation gap is varied from ~1 μm to ~5 μm, and then from ~5 μm back to ~1 μm, in 100 nm steps, with a dwell time of ~15 s per step. Next, another hold test is conducted (again, over a period of ~20 min.), followed by another ramp test. This procedure allows for the systematic characterization of both advancing and receding contacts over multiple test cycles. The high-precision nanopositioning stage is an NPXY100Z100A nanopositioner operated by a C300 controller (nPoint, Inc.), and the stage control, interferogram image processing, and data analysis were done using custom scripts in Matlab®, MathWorks, Inc.

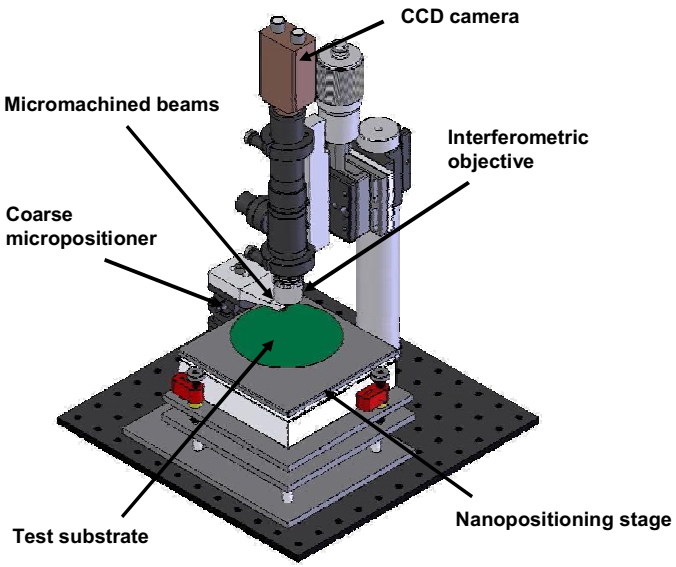

Figure 1. Test apparatus, with key components marked.

Fracture mechanics framework

To relate the measured beam profiles and contact lengths to the work of adhesion and work of separation, the Griffith energy-balance approach (7) was employed. A deformed beam in adhesive contact with an undeformed substrate (Figure 2) is the system considered, and the unbonded region beneath the beam is treated as a crack, with the line separating the bonded and unbonded potions of the beam as the crack front. The governing equation for Griffith-based fracture mechanics is:

$$\frac{\partial(W-U)}{\partial A}=\frac{\partial \Gamma}{\partial A} \qquad [1]$$

where W is the work done on the system by an externally-applied load, U is the strain energy stored in the beam, Γ is the energy of the unbonded surfaces, and A is the unbonded area. The left-hand side of the expression is known as the strain energy release rate (G), and the right-hand side of the expression is typically taken to be the work of adhesion (W_{adh}), which represents the resistance to interfacial debonding. The equilibrium condition (Equation 3) can be more succinctly expressed as:

$$G = W_{adh} \qquad [2]$$

In our experimental setup, no externally-applied loads are involved during testing, so $W = 0$, and G simply reflects the change in internal strain energy per area. Furthermore, we consider the possibility that the work of adhesion (measured when a crack recedes) may differ from the work of separation (measured as a crack advances); therefore, we make a distinction between the work of adhesion W_{adh} and the work of separation W_{sep}, modifying the equilibrium equation [2] as follows:

$$G = W_{adh} \text{ for a receeding contact}$$
$$G = W_{sep} \text{ for an advancing contact} \qquad [2]$$

To calculate G for our inclined beam apparatus, Euler-Bernoulli beam theory is used to relate the deformed beam profile to the strain energy stored in the beam. The following analytical expression is the result:

$$G = -\frac{dU_E}{dA} = -\left(\frac{1}{b}\right)\frac{dU_E}{da} = \frac{Eh^3}{6a^4}(\varphi a - 3s)^2, \qquad [3]$$

where E, b, and h are the Young's modulus, width, and thickness of the beam, respectively, φ is the angle of incline of the beam at its base, s is the separation gap between the base of the beam and the test substrate, and a is the crack (unbonded) length (Figure 2). Thus, by measuring s and a during an experiment, we can directly determine G, and Equation [2] can then be used to determine the work of adhesion (or separation) between the contacting surfaces.

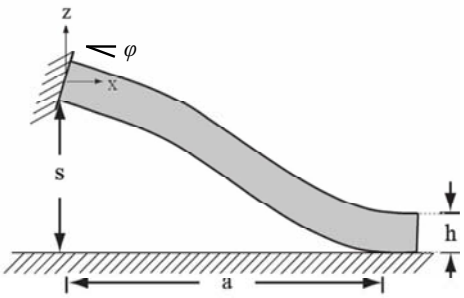

Figure 2. Schematic of a deformed beam in adhesive contact with a test substrate. The separation gap (s) is varied and the crack length (a) is measured during testing.

Specimen Fabrication and Preparation

Si chips with integrated beam arrays (r.m.s. roughness ~0.3 nm) were fabricated using commercial silicon-on-insulator (SOI) substrates (IceMos Technology). Briefly, the fabrication process consists of patterning the beam-array geometry using photolithography, using a deep reactive ion etching process to fully define the beams, and etching away portions of the handle silicon using potassium hydroxide (while leaving the chips in tact). After the fabrication process, the wafers were stored in dry nitrogen and individual chips were released from the wafer prior to testing.

Once released, each test chip and test substrate were cleaned using a two-step process (1). First, the samples were submerged in a hydrofluoric (HF) acid bath (HF:DI water 1:1) to remove oxides from the surfaces. Second, a piranha solution (H_2SO_4:H_2O_2 3:1) was used to both remove contamination and to grow a fresh, chemical oxide on the surfaces of the beams and test substrate. This renders the surfaces hydrophilic (water contact angle ~0º) and presumably OH-terminated (1). Immediately after cleaning, the chip and substrate were rinsed in DI water, and purified nitrogen was used to blow the

samples dry. The chip was then glued to the chip holder, the sample was adhered to the stage plate, and both were stored in a clean bench to allow the glue to dry prior to testing.

Results and Discussion

Figure 3 displays two example plots from a ramp test conducted at ~15% RH. Figure 3(a) shows how the crack length (a) changes while the separation gap (s) is systematically varied. The separation portion of the curve (diamonds) is flat initially (s ~1 μm), demonstrating that the strain energy in the beam needs to increase beyond its initial equilibrium value before the crack can advance. The initial behavior transitions into a monotonically-increasing region where the crack advances as s is increased to its largest value of ~5 μm. The adhesion portion of the curve (squares) begins when s is decreased, which is also initially flat due to the crack front failing to recede immediately. At a separation gap of ~2.5 μm, the crack begins to recede, and this recession continues until the ramp test is completed (with s returning to ~1 μm). Figure 3(b) shows the result of applying equation [3] to the data plotted in Figure 3(a). Initially, G increases due to s increasing without crack movement. At s ~1.25 μm, the crack advances, and G drops from ~100 mJ/m^2 to ~75 mJ/m^2. W_{sep} is taken to be the highest value that G achieves, as it corresponds to the energy release rate required to propagate a crack through the Si-Si interface. The crack continues to advance, with G remaining nearly constant, until s reaches ~5 μm. The adhesion portion of the G curve exhibits an initial monotonically-decreasing region, due to the decrease in s without a change in a. When the crack does recede, G remains constant at ~14 mJ/m^2. This value of G = 14 mJ/m^2 is taken to be W_{adh}.

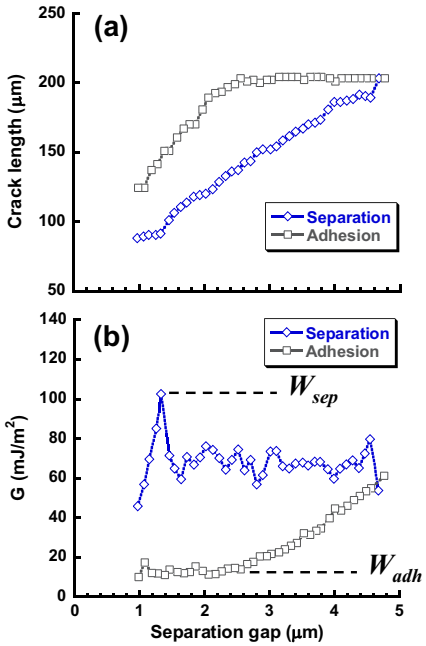

Figure 3. Example results from a test conducted at ~15% RH in a nitrogen background. (a) Crack length versus separation gap. (b) Calculated values of G corresponding to the data shown in (a).

Figure 4 displays the compiled results from ramp tests conducted at ~15% RH. Each value plotted represents the average of 5 beams tested, with the error bars corresponding to the standard errors. Comparing the results from hold #1 with ramp #1, initial value of W_{adh} measured during hold #1 is found to be less than half of the initiation value for W_{sep} measured during ramp #1. Furthermore, significant and repeatable hysteresis in W is observed when comparing the separation and adhesion values for both ramp #1 and ramp #2, with W_{adh} becoming lower (~ 11 mJ/m^2) than its value of ~35 mJ/m^2 measured during hold #1.

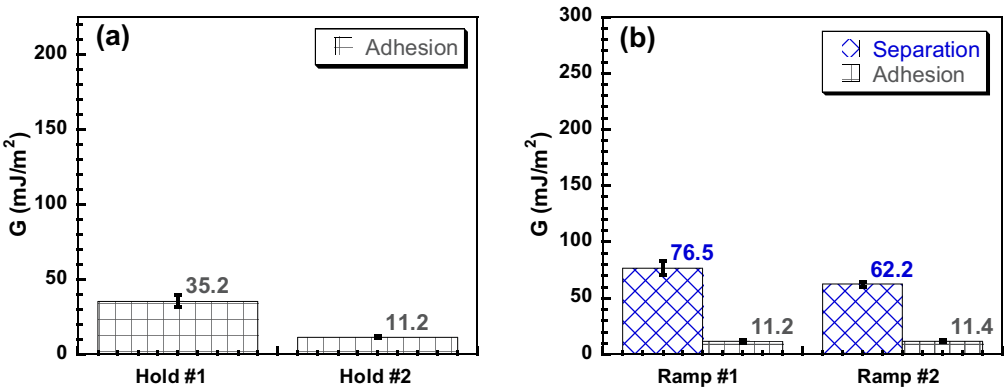

Figure 4. Results from tests conducted at ~15% RH. (a) W_{adh} measured during the hold tests. (b) W_{sep} and W_{adh} values measured during the advancing and receding portions, respectively, of the ramp tests.

Figure 5 displays the results from ramp tests conducted at ~50% RH. Each value plotted represents the average of 8 beams tested. Similarly to what was observed at ~15% RH, the initial value of W_{adh} is found to be significantly less than the initiation value for W_{sep}. Additionally, the hysteretic behavior is also observed in G during both ramp tests. In contrast to the tests conducted at 15% RH, however, the values for both W_{sep} and W_{adh} for all tests at 50% RH are significantly larger than those measured at ~15% RH. A similar difference between work of adhesion and work of separation was observed in the wafer-level experiments reported in (8).

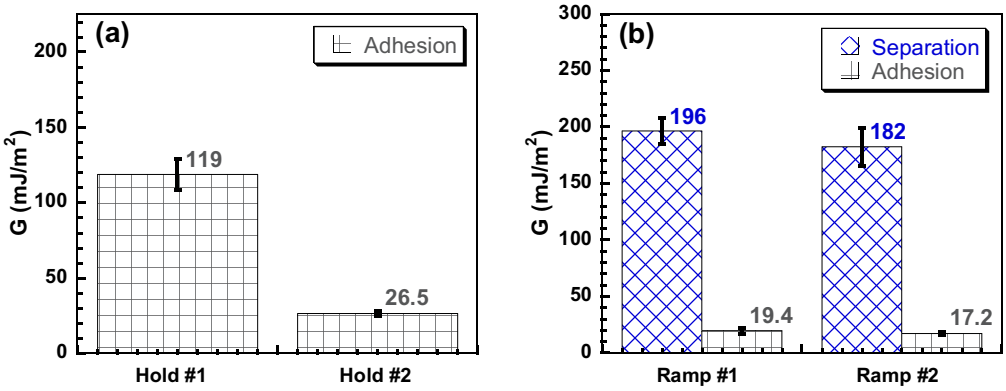

Figure 5. Results from tests conducted at ~50% RH. (a) W_{adh} measured during the hold tests. (b) W_{sep} and W_{adh} values measured during the advancing and receding portions, respectively, of the ramp tests.

The surface energy hysteresis observed in the ramp tests at both ~15% and ~50% can be explained by understanding the relative contributions of van der Waals forces, OH (i.e. hydrogen) bonding due to the presence of water, and OH bonding between terminal hydroxyl groups on the Si surfaces. Tractions due to ubiquitous van der Waals forces, unless screened by the presence of water within the contact, would contribute equally to the surface forces experienced by all interfaces studied here (with constant nominal surface roughness and surface chemistry). OH bonding from water molecules, if present at the crack front, would contribute equally to the tractions at the crack front when the crack advances and recedes, with the amount water on the surface being dependent upon on the humidity level (e.g., at a higher RH, a thicker layer of water would condense on the surface). Therefore, stronger OH bonds (i.e., between hydroxyl groups terminating the Si surfaces) that are able to form only when the surfaces are brought into intimate contact give rise to the higher work of separation values, and the weaker forces (due van der Waals interactions and OH bonding from water molecules), which can act over larger separation distances, are responsible for the tractions that initially adhere and re-adhere the beams to the test substrate. Thus, the work required to separate the surfaces includes the energy for breaking the stronger terminal hydroxyl bonds, whereas the work of adhesion of the surfaces does not include the energy for forming the stronger bonds. Additionally, the process of making and breaking these stronger bonds is reversible due the noncovalent nature of the bonding and the continual presence of van der Waals forces and water molecules.

The increase in the work of adhesion measured at ~50% RH above that measured at ~15% can be understood by recognizing that the water molecules play a larger role at the higher humidity level. In a low-RH environment, the water coverage on a surface will be fractional (depending on the surface roughness and surface energy). Above a threshold RH (~70% RH for smooth surfaces (9)), a complete monolayer of water is expected to cover the surface. The observed increase in the work of adhesion at ~50% RH is therefore hypothesized to be due to the additional tractions imparted at the crack front by the increased surface concentration of water molecules. Furthermore, the significantly-larger

values for the work of separation measured at ~50% RH suggest that the additional water molecules facilitate the formation of stronger bonds across the interface.

Ongoing research is aimed at testing these hypotheses in order to firmly establish the mechanism of adhesion hysteresis for these systems.

Conclusions

A novel test apparatus has enabled us to characterize the adhesion and separation behavior of Si-Si microscale contacts, and we have quantified the work of adhesion and work of separation in controlled-humidity environments. We observe significant and repeatable hysteresis in our ramp tests, and we can understand this in terms of stronger, reversible OH bond formation within the contact. Additionally, we observe a significant RH dependence on the work of adhesion and separation, due to the role that water plays in both increasing the work of adhesion and facilitating the formation of stronger bonds within the contact. The work here demonstrates the significance of measuring the full range of adhesion-separation behavior, and will enable detailed characterization of a wider range of material pairs than those studied previously.

Acknowledgments

This work was supported by AFOSR-MURI FA9550-08-1-0337 and NSF grant CMMI-#0845294.

References

1. A. Plossl and G. Krauter, *Materials Science and Engineering R: Reports*, **R25**, 1 (1999).
2. J. B. Lasky, *Applied Physics Letters*, **48**, 78 (1986).
3. M. A. Schmidt, *Proceedings of the IEEE*, **86**, 1575 (1998).
4. W. P. Maszara, G. Goetz, A. Caviglia and J. B. McKitterick, *Journal of Applied Physics*, **64**, 4943 (1988).
5. M. P. de Boer and T. A. Michalske, *Journal of Applied Physics*, **86**, 817 (1999).
6. F. W. DelRio, M. L. Dunn and M. P. de Boer, *Scripta Materialia*, **59**, 916 (2008).
7. G. C. Sih and H. Liebowitz, in *Fracture, An Advanced Treatise Vol. 2*, p. 68, Academic Press, London, UK (1968).
8. K. T. Turner and S. M. Spearing, *Proceedings of the Royal Society A - Mathematical Physical and Engineering Sciences*, **462**, 171 (2006).
9. D. J. Cole, M. C. Payne, G. Csanyi, S. M. Spearing and L. C. Ciacchi, *Journal of Chemical Physics*, **127**, 204704 (2007).